

1

Supporting information for

2 **Trace arsenic analysis in edible seaweeds by a miniature in-situ dielectric barrier discharge**

3 **microplasma optical emission spectrometry based on gas phase enrichment**

4 Yaru Zhang,^{a,b} Xuefei Mao,^b Di Tian,^{a*} Jixin Liu,^{b,c*} Chunsheng Li^{a*}

5 ^a College of Instrumentation & Electrical Engineering, Jilin University, Changchun 130023, China

6 ^b Institute of Quality Standard and Testing Technology for Agro-products, Chinese Academy of Agricultural

7 Sciences, and Key Laboratory of Agro-food Safety and Quality, Ministry of Agriculture and Rural Affairs,

8 Beijing 100081, China

9 ^c Beijing Ability Technique Company, Limited, Beijing 100081, China

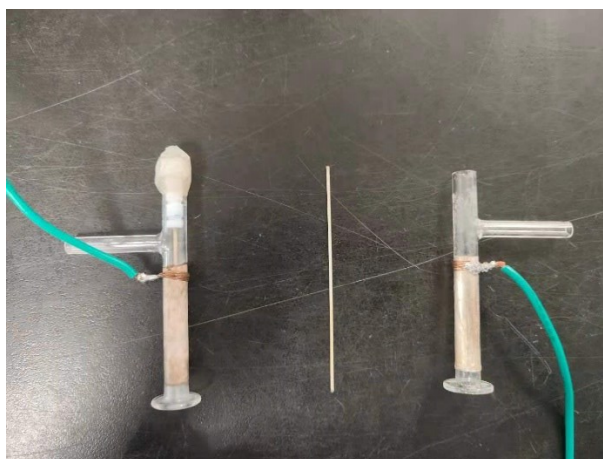
10 Corresponding authors: Tel: +86-10-82106523, Fax: +86-10-82106523.

11 E-mail address: tiandi@jlu.edu.cn (D. Tian); ljx2117@gmail.com (J. X. Liu); lies@jlu.edu.cn (C. S. Li)

12

13 1. Electrode fabrication process

14 The electrode fabrication process using silver paste is described as follows: High temperature sintered
15 conductive silver paste, which has good adhesion to quartz material and is suitable for the electrode printing
16 of various electronic components, is used for DBD electrodes. First, the silver paste is evenly coated on the
17 outer surface of DBD's outer quartz tube and the inner surface of DBD's inner quartz tube. After that, the
18 DBD coated with silver paste is placed in a hot bellows set to 100°C for an hour to remove bubbles from silver
19 paste. The DBD coated silver paste is then placed in a muffle oven at 650°C for an hour to sinter the silver
20 paste onto the quartz surface. The photos of silver-coated DBD, DBD's inner quartz tube and outer quartz tube
21 were as shown in Fig.S1.



22

23 **Fig.S1** The photos of silver-coated DBD, DBD's inner quartz tube and outer quartz tube.

24 2. Background correction method

25 In this paper, a background correction method is proposed to eliminate the influence of background
26 fluctuation. In this method, a baseline is fitted according to Equation (1), in which $f_{\text{Base}(i)}$ indicates the
27 intensity of point i on baseline curve, $f(i)$ indicates the intensity of point i on initial spectrum and $d_{\text{Aver}(i)}$
28 indicates the average intensity of point i and its surrounding points on initial spectrum, which is calculated as
29 Equation (2). In Equation (2), d indicates the number of point on one side on point i (in this experiment, d is

30 set as 13). After the baseline curve (f_{Base}) is obtained, another baseline (f_{base2}) is calculated by replacing $f(i)$
 31 in Equation (1) and Equation (2) with $f_{base}(i)$. The final baseline curve is obtained by replacing $f(i)$ in Equation
 32 (1) and Equation (2) with $f_{base2}(i)$. The spectrum after background correction is obtained by subtracting the
 33 final baseline curve from the initial spectrum. In addition, in order to reduce the influence of noise, Savitzky-
 34 Golay filter is performed on the spectrum after background correction. In this experiment, the window width
 35 of Savitzky-Golay filter is set as 5 points (0.4 nm) and Polynomial number is set as 2.

$$36 \quad f_{Base}(i) = \begin{cases} f(i) & f(i) < dAver(i) \\ dAver(i) & f(i) > dAver(i) \end{cases} \quad (1)$$

$$37 \quad dAver(i) = \left(\sum_{j=-d}^{j=d} f(i+j) \right) / (2*d+1) \quad (2)$$

38 3. Detail procedure of the improved peak volume algorithm

39 In this article, an improved peak volume algorithm is proposed to solve this problem, where start time
 40 point and end time point of the spectrum at each concentration are determined according to a unified judgment
 41 criteria. First, the peak area at each time point is calculated, as shown in Equation 1. Then, find the maximum
 42 peak area and name its corresponding time point index N_{max} . Subsequently, find the start time point N_{start} and
 43 end time point N_{end} as shown in the flow chart 1 and 2. The unified judgment criteria was as shown in
 44 inequation (1) and (2). Starting from the time point index N_{max} , the peak area is accumulated along the time
 45 axis to both sides point by point until the addition of the peak area at a certain time point makes the increment
 46 rate of the accumulated peak area value less than the set volume coefficient. The volume coefficient in
 47 inequation (1) and (2) has been optimized. It was found that R^2 of the standard curve was poor in the range of
 48 1-10 $\mu\text{g L}^{-1}$ when volume coefficient is lower than 0.015, possibly because more noise signal was introduced
 49 at small intensity, and when volume coefficient is higher than 0.015, the linear range becomes narrower,
 50 possibly because the larger intensity loss at higher concentration. As a result, volume coefficient of 0.015 was
 51 selected, which can automatically adopt appropriate time width at different concentration. After determining
 52 the start time point and end time point, peak volume can be calculated according to Equation 2.

$$53 \quad I_{area}(n \times \Delta t) = \sum_{\lambda=\lambda_{start}}^{\lambda=\lambda_{end}} I_n(\lambda) \quad (1)$$

$$54 \quad I_{volume} = \sum_{n=N_{start}}^{n=N_{end}} I_{area}(n \times \Delta t) \quad (2)$$

55

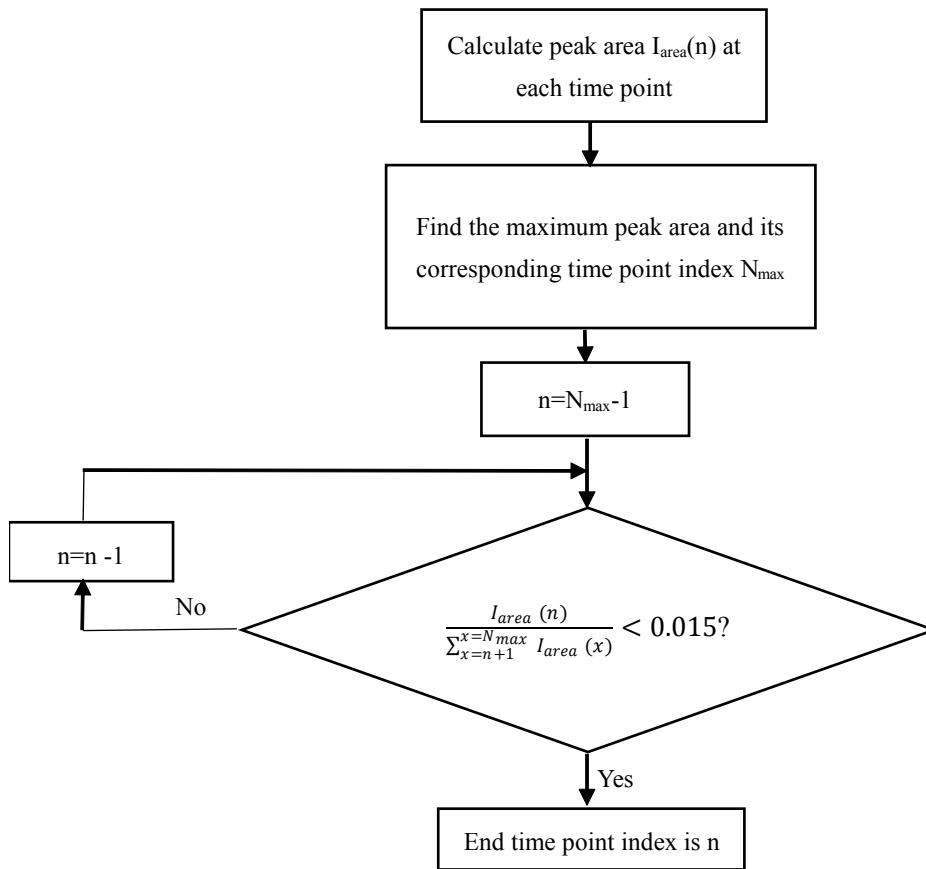
$$\frac{I_{area}(N_{start} \times \Delta t)}{\sum_{n=N_{start}+1}^{N_{max}} I_{area}(n \times \Delta t)} < volume\ coefficient \quad (1)$$

56

$$\frac{I_{area}(N_{end} \times \Delta t)}{\sum_{n=N_{max}}^{N_{end}-1} I_{area}(n \times \Delta t)} < volume\ coefficient \quad (2)$$

57 In Eq. (1), $I_{area}(n \times \Delta t)$ is the intensity calculated by peak area of the intensity-wavelength spectrum
 58 collected at $n \times \Delta t$ time. $I_n(\lambda)$ refers to the intensity-wavelength spectrum collected at $n \times \Delta t$ time. λ_{start} and
 59 λ_{end} refer to the wavelength of starting point and ending point of the peak. In Eq. (2), I_{volume} is the intensity
 60 calculated by peak volume. N_{start} and N_{end} refer to the time index of starting intensity-wavelength spectrum
 61 and ending intensity-wavelength spectrum.

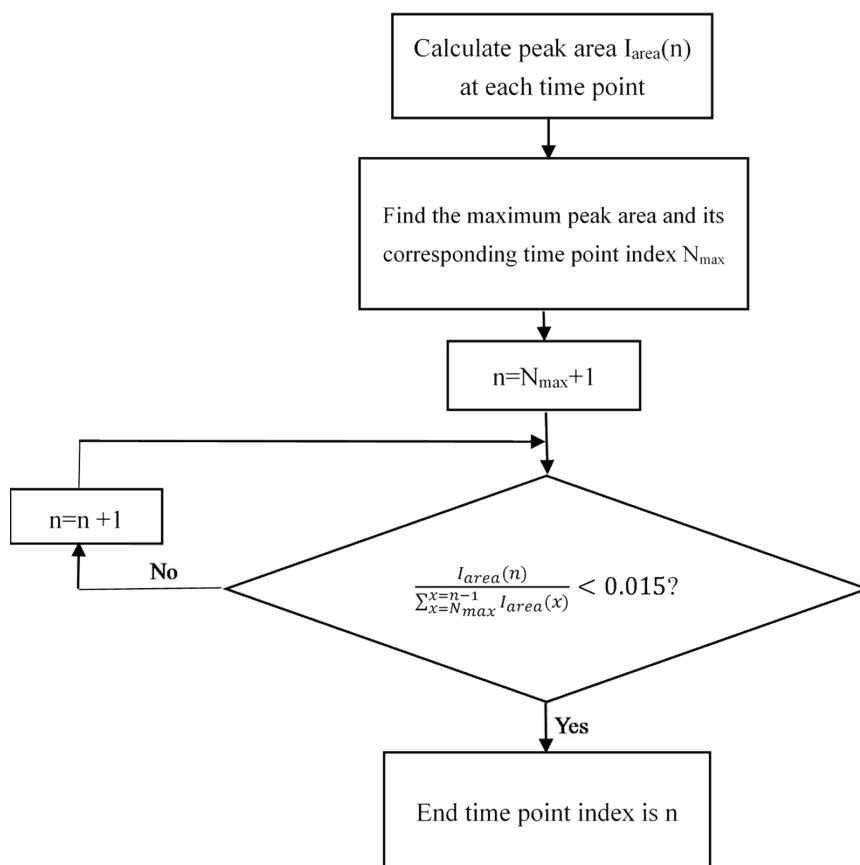
62 It is worth mentioning that the background correction was performed for each intensity-wavelength
 63 spectrum to reduce errors caused by baseline fluctuation before the comparison.



64

65

Fig.S2 Flow chart of determining start time point.



66

67

68

Fig.S3 Flow chart of determining end time point.

69 4. **The operational parameters of ICP-MS**

70

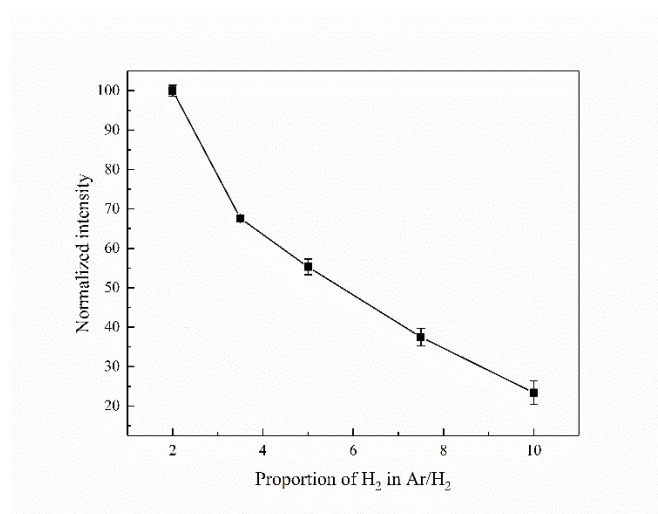
Table S1 Operational parameters of ICP-MS

Parameters	Values
Incident RF power	1150W
Sampling depth	120mm
Nebulizer Ar gas flow rate	0.8 L min ⁻¹
Cooling Ar gas flow rate	14 L min ⁻¹
Auxiliary Ar gas flow rate	1.2 L min ⁻¹
Peristaltic pump rate	30 rpm
Dwell time	10 ms
Isotopes	⁷⁵ As
Internal standard isotopes	⁷² Ge

71

72 5. **Optimization of H₂ in Ar/H₂ mixture**

73 H₂ has been validated as a crucial gas for the releasing of As from DBD's inner surface, which might
74 supply hydrogen radical to promote the atomization of As. Ar is usually employed as the working gas of
75 microplasmas as it could form stable and stronger plasma. Accordingly, a mixture gas of Ar and H₂ is
76 employed as the working gas of release step in this work. The effect of the proportion of H₂ in the mixture of
77 Ar/H₂ on the analytical signals of As was investigated. As shown in Fig.S4, As intensity decreases with the
78 increasing H₂ proportion because higher amount of H₂ would consume the energy of DBD plasma and cause
79 a decrease of its excitation capability. However, sever tailing of As releasing intensity could be observed when
80 the proportion of H₂ in Ar/H₂ is below 5%. Therefore, the proportion of 5% was selected for all subsequent
81 experiments.



82

83 **Fig. S4** Dependence of As and Sb intensities on percentage of H₂ in Ar/H₂. The intensities are normalized with
84 that in 2% H₂ set at 100, respectively.

85